Synthesis and Structure of Zirconium−Group 13 Heterobimetallic Compounds

Francis M. G. de Rege, William M. Davis, and Stephen L. Buchwald*

Department of Chemistry, Massachusetts Institute of Technology, Cambridge, Massachusetts 02139

Received April 18, 1995[⊗]

The reaction of main-group (B, Al, and Ga) alkoxides with zirconocene complexes of benzynes was used to prepare novel zirconium−group 13 heterobimetallic compounds [$R_2E(\mu\text{-}OR')(\mu\text{-}1,2\text{-aryl})Zr(\eta^5\text{-}C_5H_5)_2$] [E = B, R = Et, R′ = Me, aryl = phenyl (**1**); E = B, R = Me, R′ = Et, aryl = phenyl (**2**); E = B, R = Et, R′ = Me, aryl = 3-methoxyphenyl (**3**); E = Al, R = Et, R′ = Et, aryl = phenyl (**5**); E = Ga, R = Me, R′ = Me, aryl = 3-methoxyphenyl (**6**)] and [$(EtO)_2B(\mu\text{-}1,2\text{-naphthyl})Zr(\eta^5\text{-}C_5H_5)_2(OEt)$] (**4**). Complexes **3** and **4** have been characterized by X-ray crystallography. Compound **3** contains a dative bond from an oxygen lone pair of the methoxy ligand on the zirconium to an acceptor p-orbital on the boron atom (^{11}B NMR; δ 8.26 ppm). In contrast, the weakly Lewis acidic boron center in **4** (^{11}B NMR; δ 29.7 ppm) does not show a bonding interaction between the alkoxy ligand on the zirconium fragment and the boron center.

Introduction

Much of the current interest in main-group heterobimetallic complexes is due to their potential use as single source precursors for electronic, optical, or refractory materials.[1] Vicinally disubstituted olefins or arenes with two main-group fragments would be interesting to study as possible precursors to ceramic materials (Scheme 1), but few of these compounds are known.[2] Since we have been interested in the synthesis of novel main-group compounds *via* zirconocene-mediated routes for several years,[3] the synthesis of such main-group complexes is an attractive goal. Scheme 2 shows how this could be achieved, possibly as a one-pot procedure, in two transmetalation steps from a zirconocene complex of an alkyne or aryne. In the first step, as described by Erker,[4] a main-group compound would react with a zirconocene aryne or alkyne complex **A** giving a heterobimetallic complex **B**. In the second step, the transmetalation from zirconium to a main-group species[3,5] would then lead to the desired compounds **C**.

Scheme 1.

Scheme 2

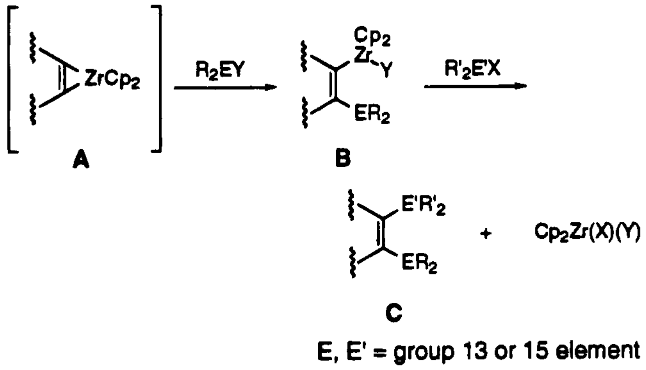

We recently reported a procedure for the preparation of zirconium−boron heterobimetallic complexes by the reaction of borates and borinates with zirconocene complexes of arynes. The most interesting aspect of these reactions was that the combination of $(EtO)_3B$ with zirconocene benzyne complexes led to a product which contained the boron fragment *ortho* to the substituent on the benzene ring. In contrast, when Et_2BOMe was used, the product observed had the boron fragment *meta* to the substituent on the benzene ring.

[⊗] Abstract published in *Advance ACS Abstracts,* September 1, 1995.

(1) (a) Cowley, A. H.; King, C. S.; Decken, A. *Organometallics* **1995,** *14,* 20. (b) Cleaver, W. M.; Späth, M.; Hnyk, D.; McMurdo, G.; Power, M. B.; Stuke, M.; Rankin, D. W. H.; Barron, A. R. *Organometallics* **1995,** *14,* 690. (c) Wells, R. L. *Coord. Chem. Rev.* **1992,** *112,* 273. (d) Jones, A. C. *J. Cryst. Growth* **1993,** *129,* 728. (e) Cowley, A. H.; Jones, R. A. *Polyhedron* **1994,** *13,* 1149. (f) Petrie, M. A.; Power, P. P. *Organometallics* **1993,** *12,* 1592. (g) Wells, R. L.; McPhail, A. T.; Self, M. F.; Laske, J. A. *Organometallics* **1993,** *12,* 3333. (h) Beachley, O. T., Jr.; Royster, T. L., Jr.; Arhar, J. R.; Rheingold, A. L. *Organometallics* **1993,** *12,* 1976.

(2) (a) Wrackmeyer, B.; Guldner, G.; Abu-Orabi, S. T. *Tetrahedron* **1989,** *45,* 1119. (b) Wang, K. K.; Chu, K. H.; Lin, Y.; Chen, J. H. *Tetrahedron* **1989,** *45,* 1105. (c) Schacht, W.; Kaufmann, D. *J. Organomet. Chem.* **1987,** *331,* 139. (d) Kaufmann, D. *Chem. Ber.* **1987,** *120,* 901. (e) Kerschl, S.; Wrackmeyer, B. *J. Chem. Soc., Chem. Commun.* **1985,** 1199. (f) Schewchuk, E.; Wild, S. B. *J. Organomet. Chem.* **1977,** *128,* 115. (g) Binger, P.; Köster, R. *J. Organomet. Chem.* **1974,** *73,* 205.

(3) (a) Buchwald, S. L.; Fisher, R. A.; Foxman, B. M. *Angew. Chem., Int. Ed. Engl.* **1990,** *29,* 771. (b) Fisher, R. A.; Nielsen, R. B.; Davis, W. M.; Buchwald, S. L. *J. Am. Chem. Soc.* **1991,** *113,* 165. (c) Spence, R. E. v. H.; Hsu, D. P.; Buchwald, S. L. *Organometallics* **1992,** *11,* 3492. (d) Hsu, D. P.; Warner, B. P.; Fisher, R. A.; Davis, W. M. *Organometallics* **1994,** *13,* 5160. (e) Buchwald, S. L.; Fisher, R. A.; Davis, W. M. *Organometallics* **1989,** *8,* 2082.

(4) (a) Albrecht, M.; Erker, G.; Nolte, M.; Kruger, C. *J. Organomet. Chem.* **1992,** *427,* C21. (b) Erker, G.; Albrecht, M. *Organometallics* **1992,** *11,* 3517. (c) Erker, G.; Albrecht, M.; Krüger, C.; Werner, S. *J. Am. Chem. Soc.* **1992,** *114,* 8531. (d) Erker, G.; Noe, R.; Wingbermühle, D. *Chem. Ber.* **1994,** *127,* 805. (e) Erker, G.; Noe, R.; Wingbermühle, D. *Angew. Chem., Int. Ed. Engl.* **1993,** *32,* 1213.

(5) (a) Fagan, P. J.; Nugent, W. A.; Calabrese, J. C. *J. Am. Chem. Soc.* **1994,** *116,* 1880. (b) Fryzuk, M. D. *Chemica Scripta* **1989,** *29,* 427. (c) Cole, T. E.; Quintanilla, R. *J. Org. Chem.* **1992,** *57,* 7366. (d) Deloux, L.; Skrzypczak-Jankun, E.; Cheesman, B. V.; Srebnik, M. *J. Am. Chem. Soc.* **1994,** *116,* 10302. (e) Negishi, E.; Takahashi, T. *Synthesis* **1988,** 1. (f) Zablocka, M.; Igau, A.; Majoral, J. P.; Pietrusiewicz, K. M. *Organometallics* **1993,** *12,* 603. (g) Boutonnet, F.; Dufour, N.; Straw, T.; Igau, A.; Majoral, J. P. *Organometallics* **1991,** *10,* 3939.

0276-7333/95/2314-4799$09.00/0

Table 1. Results for the Synthesis of Zirconium–Main-Group Aromatic Compounds

Compound	Structure	Isolated Yield
1	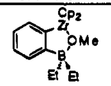	78%
2	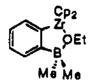	54 %
3	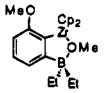	52%
4	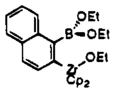	55 %
5	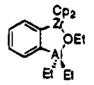	44%
6	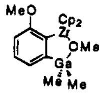 a 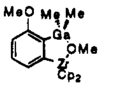 b	52%[a]

[a] Isolated as an inseparable mixture of **6a** and **6b** in a ratio of 65:35.

Thus, the regioselectivity could be manipulated by the choice of boron reagent used. It was shown that these intermediate complexes could be converted, without isolation, to the corresponding halophenols, resulting in an overall regiospecific synthesis of halophenols.[6]

Herein we report, for the first time, the isolation and characterization of several of the complexes (**1**–**4**, Table 1) which were intermediates in our procedure for the synthesis of halophenols. The structures of **3** and **4**, as determined by X-ray crystallography, are also reported. In addition, we have isolated the aluminum (**5**) analogue of **1** and gallium (**6**) analogue of **3**.

Results and Discussion

The zirconium–group 13 heterobimetallic compounds that were prepared are listed in Table 1. These were all made by treating a group 13 alkoxide with an appropriate zirconocene complex of an aryne.[7] The products were obtained in 80–90% yield (^{1}H NMR) and were isolated in yields of 44–78% (based on Cp_2ZrPh_2 for **1**, **2**, and **5** and based on $Cp_2Zr(Me)Cl$ for **3**, **4**, and **6**).

Treatment of **7**, generated *in situ* from diphenylzirconocene, with either Et_2BOMe or Me_2BOEt in THF or benzene, leads, respectively, to the isolation of **1** (78%) or **2** (54%) (eqs 1 and 2). Similarly, **3** (52%) and **4** (55%) were prepared from zirconocene–aryne complexes and Et_2BOMe or $(EtO)_3B$ (eqs 3 and 4). It was not possible to isolate the benzene analog of **4** in pure form (it was ~80% pure as estimated by ^{1}H NMR).

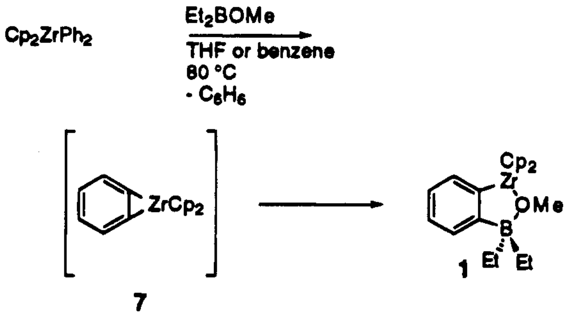

1)

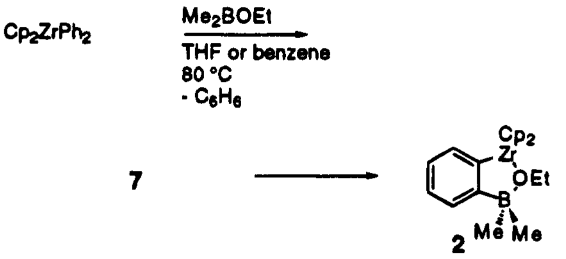

2)

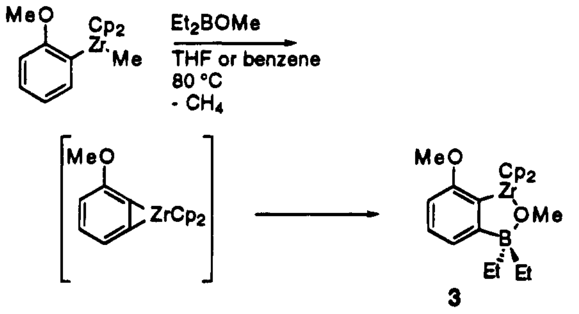

3)

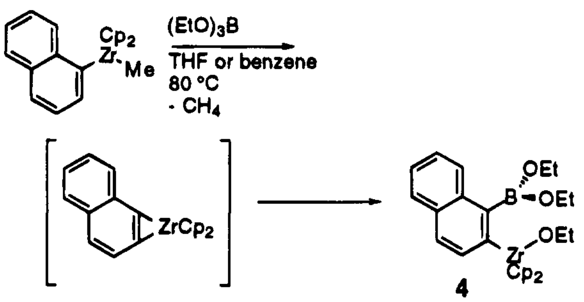

4)

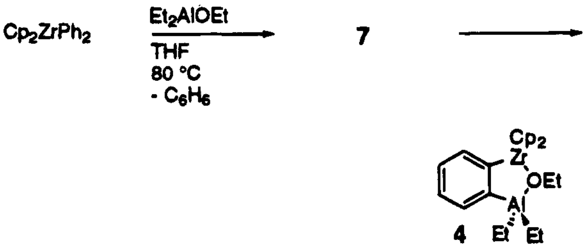

5)

While the reactions of borates and borinates with **7** proceeded in benzene, the reaction of Et_2AlOEt and **7** needs a more coordinating solvent and was carried out in THF (eq 5). We attribute this to the strong heteroatom mediated bridging that occurs in aluminum complexes.[8] These highly bridged structures would make the aluminum-oxygen bond less likely to react with the zirconium-carbon bond of **7** based on steric and electronic grounds. In a coordinating solvent such as THF, the oligomers are broken up by the interaction of THF with the aluminum center.

When we performed the reaction of Me_2GaOMe with **7**, we found that ligand exchange occurs between the phenyl ligands on Cp_2ZrPh_2 and the methoxy ligands

---

[6] de Rege, F. M. G.; Buchwald, S. L. *Tetrahedron* **1995**, *51*, 4291.

[7] Broene, R. D.; Buchwald, S. L. *Science* **1993**, *261*, 1696.

[8] (a) Eisch, J. J. In *Comprehensive Organometallic Chemistry*, Wilkinson, G., Ed.; Pergamon: New York, 1982; Vol. 1; pp 555–682. (b) Odom, J. D. In *Comprehensive Organometallic Chemistry*, Wilkinson, G., Ed.; Pergamon: New York, 1982; pp 253–310.

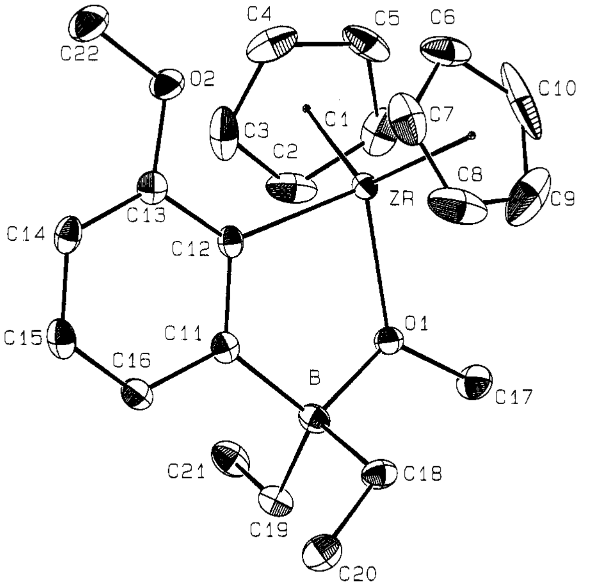

Figure 1. ORTEP drawing of **3** (thermal ellipsoids at 35% probability).

on Me_2GaOMe. We therefore generated the PMe_3 adduct of the zirconocene–benzyne complex, **7**·PMe_3, which was then treated with Me_2GaOMe (eq 6). Unlike the reaction with boron reagents, the reaction was not very regioselective, giving a 52% isolated yield of **6** as a 65:35 mixture of isomers **a** and **b**.[9]

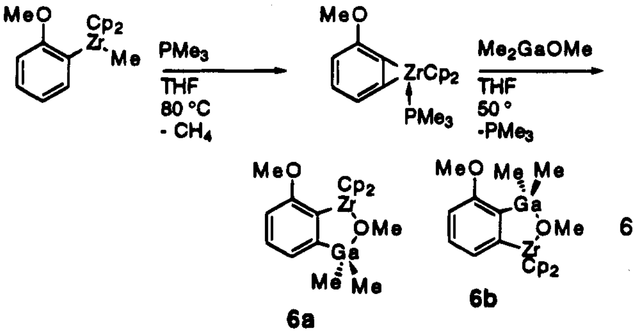

6a **6b**

6)

Single crystals of **3**, suitable for X-ray structure determination, were obtained by the slow diffusion of pentane into a saturated solution of **3** in toluene. An ORTEP diagram of **3** is shown in Figure 1, and selected bond lengths and bond angles of **3** are given in Table 2.

For comparison to **3**, the structure of **4** was also determined by X-ray crystallography. Single crystals of **4** were obtained by the diffusion of pentane into a saturated solution of **4** in toluene at −40 °C over a 2 week period. There are two fragments in the unit cell of **4** where one fragment (fragment 2) has some disorder. An ORTEP diagram of **4** is shown in Figure 2, while Table 3 lists some important bond lengths and angles of **4** taken from fragment 1. The corresponding values for fragment 2 do not vary from these values significantly.

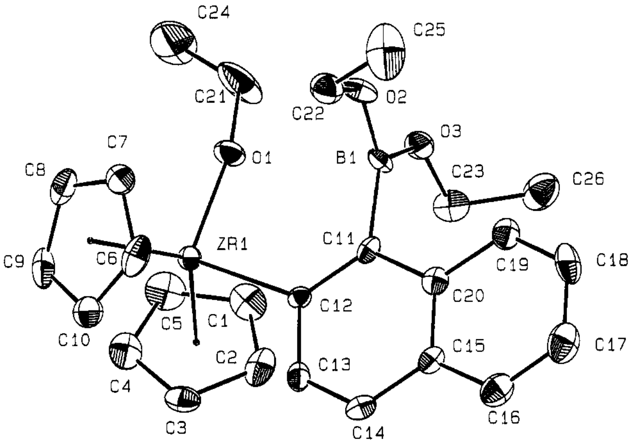

Figure 2. ORTEP drawing of **4** (thermal ellipsoids at 35% probability).

Table 2. Selected Bond Lengths and Angles for 3

atoms	length (Å)	atoms	angle (deg)
Zr–O(1)	2.104(2)	O(1)–Zr–C(12)	83.2(1)
Zr–C(12)	2.231(4)	Zr–C(12)–C(13)	130.2(3)
B–O(1)	1.622(5)	O(1)–B–C(11)	104.5(3)
B–C(18)	1.635(6)	O(1)–B–C(18)	107.4(3)
B–C(19)	1.627(6)	O(1)–B–C(19)	107.9(3)
B–C(11)	1.629(6)	C(11)–B–C(18)	112.4(3)
O(1)–C(17)	1.432(5)	C(11)–B–C(19)	113.8(3)
O(2)–C(22)	1.423(5)	C(18)–B–C(19)	110.3(3)
C(11)–C(12)	1.412(5)	C(11)–C(12)–C(13)	120.0(3)
C(12)–C(13)	1.406(5)	C(12)–C(13)–C(14)	122.2(4)
C(13)–C(14)	1.381(6)	C(13)–C(14)–C(15)	118.0(4)
C(14)–C(15)	1.388(6)	C(14)–C(15)–C(16)	121.3(4)
C(15)–C(16)	1.377(6)	C(11)–C(16)–C(15)	121.9(4)
C(16)–C(11)	1.420(6)	Zr–O(1)–B	116.8(2)
		Zr–O(1)–C(17)	124.9(2)
		B–O(1)–C(17)	117.5(3)

Table 3. Selected Bond Lengths and Angles for 4, Fragment 1

atoms	length (Å)	atoms	angle (deg)
Zr–O(1)	1.916(5)	O(1)–Zr–C(12)	97.9(2)
Zr–C(12)	2.302(6)	Zr–C(12)–C(13)	118.4(9)
B–O(1)	2.84	Zr–O(1)–C(21)	160.2(6)
B–O(2)	1.357(9)	O(2)–B–C(11)	124.0(7)
B–O(3)	1.353(9)	O(3)–B–C(11)	123.5(7)
B–C(11)	1.60(1)	O(2)–B–O(3)	112.2(6)
O(1)–C(21)	1.36(1)	C(20)–C(11)–B	116.6(6)
O(2)–C(22)	1.417(9)	C(11)–C(12)–C(13)	117.3(6)
C(3)–C(23)	1.416(9)	C(12)–C(13)–C(14)	123.8(6)
C(11)–C(12)	1.391(9)	C(13)–C(14)–C(15)	119.7(6)
C(12)–C(13)	1.423(9)	C(14)–C(15)–C(16)	121.4(7)
C(13)–C(14)	1.368(9)	C(15)–C(16)–C(17)	120.7(7)
C(14)–C(15)	1.409(9)	C(16)–C(17)–C(18)	120.7(7)
C(15)–C(20)	1.407(9)	C(17)–C(18)–C(19)	119.8(7)
C(15)–C(16)	1.411(9)	C(18)–C(19)–C(20)	121.5(7)
C(16)–C(17)	1.35(1)	C(11)–C(20)–C(15)	120.6(6)
C(17)–C(18)	1.40(1)	C(11)–C(20)–C(19)	121.9(6)
C(18)–C(19)	1.37(1)	C(15)–C(20)–C(19)	117.5(6)
C(19)–C(20)	1.423(9)		
C(20)–C(11)	1.450(9)		

Figure 3 highlights some of the structural features of **3** and **4**. The B–O(1) bond length in **3** of 1.622(5) Å is slightly longer than the sum of covalent radii (1.54 Å),[10] consistent with a dative interaction. In contrast, the B–O(1) distance in **4** is greater than 2.8 Å, implying that there is no bond. In **3**, the coordination environment of boron is almost tetrahedral where the average bond distance from boron to the carbon atoms bonded to it is 1.630(6) Å, a characteristic value for tetracoor-

---

[9] A difference NOE experiment supported the assignment of isomers. A 1.8% NOE was found in compound **6a** between the methyl groups on the gallium atom and the ortho proton on the aromatic ring. A 1.0% NOE was found in compound **6b** between the methyl groups on the gallium and the ortho methoxy group.

[10] (a) Pelter, A.; Smith, K. In *Comprehensive Organic Chemistry*, Jones, D. N., Ed.; Pergamon: New York, 1979; Vol. 3, pp 915–924. (b) Nöth, H.; Staude, S.; Thomann, M.; Kroner, J.; Paine, R. T. *Chem. Ber.* **1994**, *127*, 1923. (c) Rettig, S. J.; Trotter, J.; Kliegel, W.; Nanninga, D. *Can. J. Chem.* **1978**, *56*, 1676.

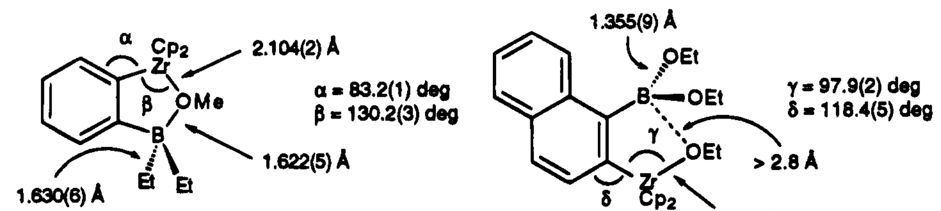

3 **4**

Figure 3.

Scheme 3

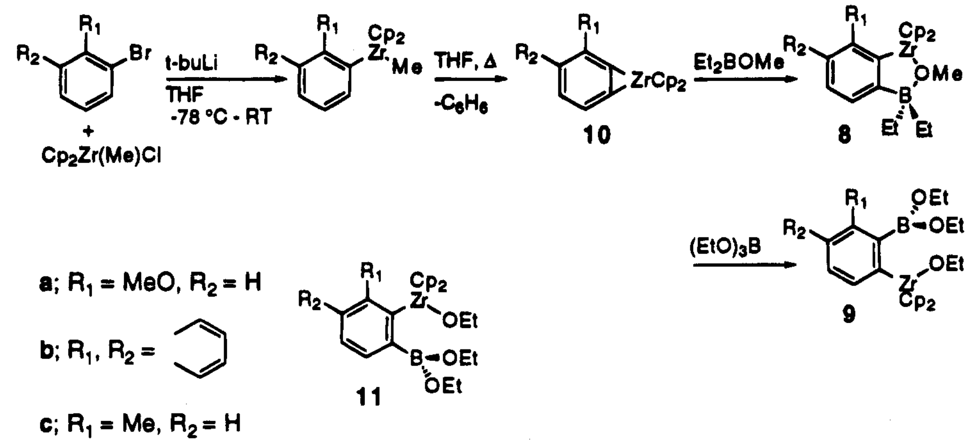

dinate boron compounds (typically 1.62–1.65 Å).[8b] The average boron–oxygen (ethoxy ligands) bond distance in **4** is 1.355(9) Å, which is a typical value for a tricoordinated alkoxy boron compound (1.38 Å for $(EtO)_3B$). The geometry of **3**, where the aryl ring, boron, zirconium, and oxygen are nearly coplanar,[11] does not allow for zirconium–oxygen multiple bonding to occur, and therefore, the Zr–O(1) bond length of 2.104(2) Å is close to that expected for a zirconium–oxygen single bond (~2.0 Å).[12] In comparison, **4** has a Zr–O(1) bond length of 1.916(5) Å implying that there may be some multiple bond character in the zirconium–oxygen bond due to π-donation from an oxygen lone pair to an empty orbital on zirconium. The C(12)–Zr–O(1) bond angle (γ, Scheme 3) in **4** of 97.9(2)° is in the range expected for a d^0 Cp_2ZrR_2 complex,[13] while the corresponding angle in **3** (β, Scheme 3) of 83.2(1)^0 is smaller than theoretically expected but close to that seen for other oxazirconacycles.[14]

The solution structures of compounds **1**–**4** were probed by ^{11}B NMR. The chemical shifts indicated that the boron atoms in **1**–**3** are tetracoordinate while in **4** the boron center is tricoordinate. For comparison, the chemical shifts of these zirconium–boron complexes and some other known boron compounds are listed (Table 4). The chemical shift of compounds **1**–**3** are those of a fairly electron-rich boron center, such as a borate. This is consistent with a bridging alkoxide between the boron and zirconium in **1**–**3**. The ^1H NMR spectra of **1** and **3** show that the methylene protons are diasteriotopic, also consistent with a bridging structure. In contrast, the ^{11}B NMR chemical shift for **4** suggests a boron center that is moderately electron rich, such as a borinate. For example, the chemical shift of **4** is very similar to that of $PhB(OMe)_2$.[10a] From this, and the solid state structure, it is reasonable to assume that there is no bridging alkoxy group between the boron and the zirconium of **4** in solution.

Table 4. Representative ^{11}B Chemical Shifts

borane	δ (ppm, $\delta(BF_3{\cdot}Et_2O) = 0$)
$Li[B(Ph)_4]^a$	−16.6
$Li[B(OMe)_4]^a$	2.7
$PhB(OMe)_2^b$	28.7
1	7.13
2	1.14
3	8.29
4	29.65

[a] See ref 15. [b] See ref 10a.

The different structures seen in **1**–**3** *vs* **4** can be explained by the electronic nature of the boron center. In **4**, π-donation from an oxygen lone pair partially fills the empty p-orbital on the boron and decreases its tendency to bridge. Since no π-donation is available for **1**–**3**, the electrophilic boron center takes on an additional ligand in the form of a bridging methoxy group.

The reaction of Et_2BOMe and $(EtO)_3B$ with zirconocene complexes of substituted benzynes proceeded to give zirconium–boron complexes **8** and **9**, respectively (Scheme 3). We previously have shown that these insertion reactions are highly regioselective and that the regioisomer obtained could in most cases be controlled by the boron reagent used.[6] For the reactions of compounds containing unsaturated functional groups with **10**, the insertion reaction is also highly regioselective, but only insertion from the less hindered side of **10** occurs leading to the kinetic product.[7,16] Similarly, the reaction of Et_2BOMe with **10** gives the expected

---

(11) For the plane containing the aromatic ring, Zr, O(1), and B, the mean deviation from the plane is 0.0683 Å.

(12) Howard, W. A.; Parkin, G. *J. Am. Chem. Soc.* **1994**, *116*, 606.

(13) Lauher, J. W.; Hoffmann, R. *J. Am. Chem. Soc.* **1976**, *98*, 1729.

(14) (a) Seyferth, D.; Wang, T.; Davis, W. M. *Organometallics* **1994**, *13*, 4134. (b) Mashima, K.; Yamakawa, M.; Takaya, H. *J. Chem. Soc., Dalton Trans.* **1991**, 2851. (c) Tikkanen, W. R.; Petersen, J. L. *Organometallics* **1984**, *3*, 1651. (d) Erker, G.; Engel, K.; Atwood, J. L.; Hunter, W. E. *Angew. Chem., Int. Ed. Engl.* **1983**, *22*, 494.

(15) Nöth, H.; Vahrenkamp, H. *Chem. Ber.* **1966**, 1049.

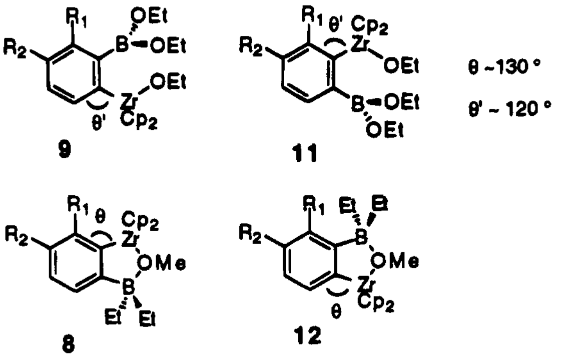

Figure 4.

Table 5. Effect of Temperature on the Product Distribution in the Reaction of 10a with $(EtO)_3B$

temp (°C)	reacn	ratio of isomers	
		11a	**9a**
25	**10a**·PMe_3 + $(EtO)_3B$	95	5
80	**10a** + $(EtO)_3B$	50	50
110	**10a** + $(EtO)_3B$	21	79

kinetic product **8**. In contrast, the reaction of $(EtO)_3B$ with **10b** or **10c** gives **9b** or **9c**, where the boron reagent ultimately approaches from the more congested side of **10**. In the reaction of $(EtO)_3B$ with **10a**, both **9a** and **11a** were obtained.

As shown in Table 5, the ratio of **9a** to **11a** depended on the temperature at which the reaction was carried out. At room temperature the reaction of **10a**·PMe_3 with $(EtO)_3B$ gave mostly **11a** (**a** to **b**, 95:5). At 110 °C the ratio is reversed (**a** to **b**, 21:79). At the intemediate temperature of 80 °C, equilibration is slow and the ratio after 1 week is 50:50. Thus the product mixture at room temperature is the kinetic one while that formed at 110 °C represents the thermodynamic distribution.

The reason that **9** and related compounds are more stable then their corresponding regioisomers (e.g., **11**) is probably steric in nature. In **11** the substituent on the aromatic ring (R_1) is close to the large zirconocene fragment, while in **9** the same substituent is positioned next to the relatively small $B(OEt)_2$ fragment (Figure 4). One might expect that the same arguments should apply in comparing the relative stabilities of **8** and **12** (Figure 4). As previously noted, however, only **8**[17] is observed when **7** is generated in the presence of Et_2-BOMe. This may be due to the methoxy group which bridges between the zirconium and boron in **8**, pulling the zirconium away from the substituent R_1, leading to a lessening of the steric interaction between R_1 and the zirconocene fragment in **8**. The boron-centered group in **12** is also effectively larger than that in **9**, since it is sp^3 hybridized, exacerbating the interaction of R_1 with the BEt_2 fragment in **12** relative to that of R_1 with the $B(OEt)_2$ fragment in **9**.

In the case of the reaction between Me_2GaOMe and **10a**·PMe_3 it is not clear why two isomers (**6a,b**) are observed. We suspected that **6a** might be favored kinetically while **6b** would predominated under thermodynamic conditions. We noticed that heating the mixture **6a,b** to higher temperatures led to a change in the ratios of **6a** to **6b** (65:35 for **a** to **b** at 50 °C, 32:68 for **a** to **b** at 110 °C) but significant decomposition to unknown products also occurred, diminishing the relevance of this observation. The structure of **6** may be important in understanding the observed isomeric distribution; unfortunately, attempts to grow single crystals of **6** or an analog suitable for X-ray crystallographic analysis have, to date, been unsuccessful.

In summary we have prepared a series of zirconium–group 13 heterobimetallic compounds by the reaction of zirconocene–aryne complexes and main-group complexes containing alkoxy ligands. The crystal structures of zirconium–boron heterobimetallic complexes **3** and **4** as well as ^{11}B NMR have shown these to have very different structures both in the solid state and in solution. The most important difference in the structures of **3** and **4** is that **3** contains a methoxy ligand bonded to boron and zirconium while **4** has no bridging alkoxide. We believe that this structural difference causes different intermolecular steric interactions in **3** and **4**, accounting, at least in part, for the different regiochemistry observed in the reactions to form these complexes.

Experimental Section

General Considerations. All reactions were carried out under an atmosphere of purified argon or nitrogen using standard Schlenk techniques. Transfer and storage of air-sensitive, moisture-sensitive, or hygroscopic materials were performed in a Vacuum Atmospheres Co. drybox under an atmosphere of nitrogen. Nuclear magnetic resonance (NMR) spectra were recorded on a Varian Unity-300 or a Varian XL-300 Fourier transform spectrometer. Melting points were determined with a Haake Buchler melting point apparatus and are uncorrected. Gas chromatography (GC) analyses were performed on a Hewlett-Packard Model 5890 gas chromatograph with a flame ionization detector and a Model 3392A integrator using a 25 m capillary column with polymethylsiloxane (Hewlett-Packard) as a stationary phase. Combustion analysis was performed by E&R Microanalytical Laboratory, Corona, NY.

Tetrahydrofuran (THF), toluene, and pentane were dried and deoxygenated by refluxing and distilling from sodium/benzophenone ketyl under an argon atmosphere. Diphenylzirconocene was prepared by the reaction of zirconocene dichloride with phenylmagnesium bromide.[18] Zirconocene methyl chloride[19] and Me_2GaOMe[20] were prepared by the published procedures. All other reagents were commercially available and used without further purification.

Preparation of $Et_2B(\mu\text{-}OMe)(\mu\text{-}1,2\text{-phenyl})ZrCp_2$ (1). A dry sealable Schlenk tube with a stirring bar was charged with diphenylzirconocene (0.376 g, 1 mmol) in a glovebox. The flask was removed from the glovebox and attached to a Schlenk line, and THF (10 mL) was added. Et_2BOMe (0.26 mL, 2 mmol) was added *via* syringe. The flask was sealed and heated in an oil bath at 80 °C for 18 h. After the reaction mixture was allowed to cool to room temperature, the volatiles were removed *in vacuo*. The crude boron–zirconium complex was redissolved in toluene (5 mL), and pure product was precipitated from the solution upon slow addition of pentane (20 mL) and cooling in an ice bath. The solvents were decanted from

---

[16] Buchwald, S. L.; Watson, B. T.; Lum, R. T.; Nugent, W. A. *J. Am. Chem. Soc.* **1987**, *109*, 7137.

[17] Compound **8c** was heated at 110 °C in THF-d_8 for 2 days, and only decomposition vs mesitylene internal standard was seen. Nothing attributable to **12** was observed.

[18] (a) Erker, G. *J. Organomet. Chem.* **1977**, *134*, 189. (b) Samuel, E.; Rausch, M. E. *J. Am. Chem. Soc.* **1973**, *95*, 6263.

[19] Wales, P. C.; Weigold, H.; Bell, P. *J. Organomet. Chem.* **1971**, *33*, 181.

[20] Coats, G. E.; Hayter, R. G. *J. Am. Chem. Soc.* **1953**, 2519.

the solids *via* cannula filtration, and the product was washed twice with cold pentane (10 mL). Residual solvents were removed *in vacuo* to give **1**, 0.310 g (78%), as a bright yellow powder: ^{1}H NMR (300 MHz, CD_2Cl_2) δ 0.53 (m, 4H), 0.71 (t, J = 7.2 Hz, 6H), 3.16 (s, 3), 6.30 (s, 10H), 6.91 (m, 3H), 7.15 (d, J = 6.3 Hz, 1H); ^{13}C NMR (300 MHz, THF-d_8) δ 11.66, 15.33 (broad), 52.71, 114.85, 124.09, 125.14, 133.75, 135.69, 193.80; ^{11}B NMR (300 MHz, C_6D_6, $BF_3{\cdot}OEt_2$ ext. ref.) δ 7.13; mp 118–124 °C. Anal. Calcd for $C_{21}H_{27}OZrB$: C, 63.46; H, 6.85. Found: C, 63.30; H, 6.63.

Preparation of $Me_2B(\mu$-OEt)(μ-1,2-phenyl)$ZrCp_2$ (2). Compound **2** was made in a similar fashion as **1** except that Me_2BOEt (0.28 g, 2 mmol) was used instead of Et_2BOMe. The yield for **2** was 0.207 g (54%) of a bright yellow powder: ^{1}H NMR (300 MHz, CD_2Cl_2) δ −0.11 (s, 6H), 1.24 (t, J = 7.0 Hz, 3H), 3.83 (q, J = 7.2 Hz, 2H), 6.16 (s, 10H), 6.88 (dd, J = 7.2 Hz, 1H), 6.93 (dd, J = 7.2 Hz, 1H), 7.16 (d, J = 6.9 Hz, 1H), 7.20 (d, J = 6.6 Hz, 1H); ^{13}C NMR (300 MHz, THF-d_8) δ 11.05 (broad), 18.40, 64.86, 113.43, 124.65, 125.84, 134.75, 136.02, 192.73; ^{11}B NMR (300 MHz, C_6D_6, $BF_3{\cdot}OEt_2$ ext. ref.) δ 1.14; mp 146–147 °C. Anal. Calcd for $C_{20}H_{25}OZrB$: C, 62.62; H, 6.57. Found: C, 62.30; H, 6.35.

Preparation of $Et_2B(\mu$-OMe)(μ-1,2-(3-methoxyphenyl))-$ZrCp_2$ (3). A dry sealable Schlenk tube was charged with zirconocene (methyl) chloride (1.088 g, 4 mmol) in a glovebox. The flask was removed from the glovebox and attached to a Schlenk line, and THF (20 mL) was added. The flask was then charged with 2-bromoanisole (0.50 mL, 4 mmol) and cooled to −78 °C. Using a gastight syringe, *tert*-butyllithium (3.6 mL, 1.7 M in pentane, 6 mmol) was added. After 15 min, the flask was removed from the −78 °C bath and allowed to warm to room temperature. Et_2BOMe (1.05 mL, 8 mmol) was added *via* syringe, and the flask was sealed and then heated in an oil bath for 18 h at 80 °C. After the reaction mixture was allowed to cool to room temperature, the volatiles were removed *in vacuo*. Residual THF was removed from the crude product by adding toluene (10 mL) and removing this under vacuum. The product was dissolved in toluene (10 mL) and the resulting solution cannula filtered from the solid impurities to a round bottom Schlenk flask. The toluene was removed *in vacuo* to give a solid which was dissolved in a minimal quantity of toluene (~5 mL). Product precipitated out of the solution upon slow addition of pentane (20 mL) and cooling in an ice bath. The solvents were decanted using a cannula filter, and the remaining solid was washed twice with cold pentane (5 mL). Residual solvents were removed *in vacuo* to give 0.889 g (52%) of yellow product: ^{1}H NMR (300 MHz, C_6D_6) δ 0.94 (m, 4H), 1.20 (t, J = 7.6 Hz, 6H), 2.65 (s, 3H), 3.40 (s, 3H), 5.98 (s, 10H), 6.43 (d, J = 7.1 Hz, 1H), 7.28 (m, 2H); ^{13}C NMR (300 MHz, THF-d_8) δ 11.72, 15.26, 52.21, 54.56, 104.75, 114.65, 126.03, 127.37, 162.74, 178.04; ^{11}B NMR (300 MHz, C_6D_6, $BF_3{\cdot}OEt_2$ ext. ref.) δ 8.29; mp 149–154 °C. Anal. Calcd for $C_{22}H_{30}BO_2Zr$: C, 61.67; H, 7.06. Found: C, 61.62; H, 6.96.

Preparation of $(EtO)_2B(\mu$-1,2-naphthyl)$ZrCp_2$(OEt) (4). A dry sealable Schlenk tube was charged with zirconocene (methyl) chloride (0.544 g, 2 mmol) in a glovebox. The flask was removed from the glovebox and attached to a Schlenk line, and THF (20 mL) was added. The flask was then charged with 1-bromonaphthalene (0.28 mL, 2 mmol) and cooled to −78 °C. Using a gastight syringe, *tert*-butyllithium (1.8 mL, 1.7 M in pentane, 3 mmol) was added. After 15 min, the flask was removed from the −78 °C bath and allowed to warm to 0 °C over 20 min. $(EtO)_3B$ (0.68 mL, 4 mmol) was added *via* syringe. The flask was sealed and was then heated in an oil bath for 5 h at 50 °C. After the reaction mixture was allowed to cool to room temperature, the volatiles were removed *in vacuo*. Residual THF was removed from the crude product by the addition of toluene (10 mL) and removing this *in vacuo*. The product was dissolved in toluene (10 mL) and the resulting solution cannula filtered from the insoluble materials to a round bottom Schlenk flask where the filtrate was concentrated *in vacuo*. Crystals and powdered product were obtained from the crude product by diffusion of pentane into a concentrated solution of the product in toluene at −40 °C over 2 weeks. The solids were isolated and residual solvents were removed *in vacuo*, to yield 0.543 g (55%) of a mixture of yellow powder and crystals: ^{1}H NMR (300 MHz, C_6D_6) δ 1.03 (t, J = 7.1 Hz, 3H), 1.17 (t, J = 7.1 Hz, 6H), 3.96 (m, 4H), 4.00 (q, J = 7.0 Hz, 2H), 5.92 (s, 10H), 7.40 (m, 3H), 7.63 (d, J = 8.1 Hz, 1H), 7.81 (d, J = 8.1 Hz, 1H), 7.98 (d, J = 8.1 Hz, 1H); ^{13}C NMR (300 MHz, THF-d_8) δ 17.88, 20.79, 60.37, 69.81, 112.23, 123.48, 124.56, 125.23, 127.87, 129.15, 132.13, 136.73, 136.88, 180.68; ^{11}B NMR (300 MHz, C_6D_6, $BF_3{\cdot}OEt_2$ ext. ref.) δ 29.65; mp 115–120 °C. Anal. Calcd for $C_{26}H_{31}O_3ZrB$: C, 63.27; H, 6.33. Found: C, 63.26; H, 6.58.

Preparation of $Et_2Al(\mu$-OEt)(μ-1,2-phenyl)$ZrCp_2$ (5). A dry sealable Schlenk tube with a stirring bar was charged with diphenylzirconocene (0.376 g, 1 mmol) in a glovebox. The flask was removed from the glovebox and attached to a Schlenk line, and THF (10 mL) was added. Et_2AlOEt (0.63 mL, 1.6 M in toluene, 1 mmol) was added *via* syringe. The flask was sealed, and the solution was heated in an oil bath for 18 h at 80 °C. After the reaction mixture was allowed to cool to room temperature, the volatiles were removed *in vacuo*. Residual THF was removed from the crude product by addition of toluene (10 mL) and removing the solvent mixture under vacuum. Pentane (10 mL) was added to the crude aluminum–zirconium complex, and the flask was sonicated for 30 min leading to a brown suspension in an orange solution. The solution was cannula filtered into a round bottom Schlenk flask, and the solvents were removed under vacuum until approximately 2 mL of solution remained as well as an orange precipitate. The flask was cooled in an ice bath while the solvents were decanted from the solids. Residual solvents were removed *in vacuo* leaving 0.188 g (44%) of a light orange-brown powder: ^{1}H NMR (300 MHz, C_6D_6) δ 0.27 (m, 4H), 1.15 (t, J = 6.9 Hz, 3H), 1.35 (t, J = 8.0 Hz, 6H), 3.34 (q, J = 6.9 Hz, 2H), 5.54 (s, 10H), 7.21 (m, 2H), 7.56 (m, 1H), 7.98 (m, 1H); ^{13}C NMR (300 MHz, THF-d_8): δ 1.46 (broad), 10.36, 18.47, 67.27, 109.98, 126.55, 127.66, 133.70, 139.25, 201.81; mp 96–98 °C. Anal. Calcd for $C_{22}H_{29}OZrAl$: C, 61.79; H, 6.83. Found: C, 61.73; H, 6.90.

Preparation of $Me_2Ga(\mu$-OMe)(μ-1,2-(3-methoxyphenyl))$ZrCp_2$ (6a,b). A dry sealable Schlenk tube was charged with zirconocene (methyl) chloride (0.544 g, 2 mmol) in a glovebox. The flask was removed from the glovebox and attached to a Schlenk line, and THF (20 mL) was added. The flask was then charged with 2-bromoanisole (0.25 mL, 2 mmol) and cooled to −78 °C. Using a gastight syringe, *tert*-butyllithium (1.8 mL, 1.7 M in pentane, 3 mmol) was added. After 15 min, the flask was removed from the −78 °C bath and allowed to warm to room temperature. PMe_3 (1 mL, 10 mmol) was added to the solution *via* syringe. The flask was sealed and was then heated in an oil bath for 18 h at 80 °C. After the reaction mixture was allowed to cool to room temperature, the volatiles were removed *in vacuo*. THF (20 mL) was added to dissolve the solids, and Me_2GaOMe (0.288g, 2.2 mmol) was added to the solution. The flask was again sealed and was heated in an oil bath at 50 °C for 6 h. The flask was removed from the oil bath, and after cooling of the solution to room temperature, the solvents were removed *in vacuo*. Residual THF was removed from the crude product by addition of toluene (10 mL) and removing this under vacuum. Pentane (50 mL) was added to the product, and the flask was sonicated for 1 h. The solution was cannula filtered from the solids and concentrated to approximately 3 mL. The solution was cooled in an ice bath and decanted from the precipitates that had formed. Residual solvent was removed *in vacuo* leaving 0.477 g (52%) of an off-white powder which was a mixture of the two isomers **6a,b** in the ratio of 65:35,[9] respectively. When the reaction was run at approximately 110 °C,[21] a yield of 0.266 g (29%) was obtained where the ratio of **6a** to **6b** was 32:68. **6a**: ^{1}H NMR (300 MHz, C_6D_6) δ 0.01 (s, 6H), 3.09 (s, 3H), 3.49 (s, 3H), 5.78 (s, 10H), 6.38 (dd, J = 6.0, 3.0 Hz, 2H), 7.23 (d, J

Table 6. Crystal Data for 3 and 4

	compd	
	3	**4**
mol formula	$C_{22}H_{29}BO_2Zr$	$C_{26}H_{31}BO_3Zr$
mol wt	428.51	493.56
cryst color	orange	orange
cryst habit	prismatic	prismatic
cryst dimens, mm	0.380 × 0.320 × 0.430	0.280 × 0.410 × 0.320
cell consts		
a, Å	9.4805(8)	8.242(1)
b, Å	14.300(1)	16.628(1)
c, Å	15.204(1)	17.700(1)
α Å		89.92(3)
β, deg	101.84(2)	90.63(2)
γ, deg		90.36(3)
V, Å^3	2017.4(6)	2425.5(6)
space group	$P2_1/c$	$P\bar{1}$
Z	4	4
D_{calc}, g/cm^3	1.411	1.352
diffractometer	Enraf-Nonius CAD-4	Enraf-Nonius CAD-4
radiation	Mo Kα (0.710 69 Å)	Mo Kα (0.710 69 Å)
temp, °C	86	86
attenuator	Zr foil (factor = 17.9)	Zr foil (factor = 17.9)
take off angle, deg	2.8	2.8
scan rate, deg/min	1.9–16.5 (in ω)	1.9–16.5 (in ω)
scan width	$0.80 + 0.35 \tan \theta$	$0.80 + 0.35 \tan \theta$
$2\theta_{max}$, deg	49.9	45.1
reflcns measd	3934	7041
unique reflcns	3700	607
corrs		
Lorenz–polarization	0.87–1.19	0.94–1.05
abs	(transm factors)	(transm factors)
secondary extinctn	0.95402×10^{-7} (coeff)	0.26846×10^{-6} (coeff)
obsd reflcns	2791 ($I > 3.00\sigma(I)$)	4543 ($I > 3.00\sigma(I)$)
no. variables	236	569
R	0.039	0.049
R_w	0.041	0.052
mas/min in final diff map, e/Å^3	0.41, −0.58	0.48, −0.67
GOF	3.64	1.43

= 3.0 Hz, 1H), 7.24 (d, J = 6.0 Hz, 1H); ^{13}C NMR (300 MHz, THF-d_8) δ 7.32, 54.99, 58.29, 107.64, 128.60, 130.15, 163.10, 199.38. **6b**: ^{1}H NMR (300 MHz, C_6D_6) δ 0.08 (s, 6H), 3.15 (s, 3H), 3.43 (s, 3H), 5.66 (s, 10H), 6.42 (d, J = 7.8 Hz, 1H), 7.10 (d, J = 6.9 Hz, 1H), 7.28 (dd, J = 7.5 Hz, 2H); ^{13}C NMR (300 MHz, THF-d_8) δ 6.78, 55.22, 57.83, 106.77, 112.21, 128.43, 129.59, 166.26, 199.38. Anal. Calcd for $C_{20}H_{25}O_2ZrGa$: C, 52.41; H, 5.50. Found: C, 52.23; H, 5.57.

Preparation of $(EtO)_2B(\mu$-1,2-(3-methoxyphenyl))$ZrCp_2$(OEt) (9a, 11a). The procedure used is the same as that for **3** except that (1) $(EtO)_3B$ (0.34 mL, 2 mmol) was used instead of Et_2BOMe, (2) three different reaction temperatures were used leading to different ratios of **9a** to **11a**, and (3) the product could not be isolated cleanly and so its structure was deduced by conversion to methoxyphenol. Integration of ^{1}H NMR cyclopentadiene resonances of **9a** (δ 5.81) and **11a** (δ 6.00) was used for determination of the isomeric ratios listed in Table 5.

Temperature Dependence of the Product Ratio. These experiments were done in toluene-d_8[22] with mesitylene as an internal standard. The room-temperature reaction was done using **8a**·PMe_3 as in the synthesis of **6**, and the ratio of **9a** to **11a** observed was 5:95. The reaction run at 80 °C gave a ratio of **9a** to **11a** of 50:50 after heating for 1 week. At 110 °C, the product ratio of **9a** and **11a** was 79:21 after 18 h.

Derivatization. The reaction to synthesize **9a** and **11a** was done at 110 °C in THF.[21] The solvents were removed from the crude **9a** and **11a** products, and this was redissolved in THF. An aqueous solution of HCl (2 mL, 10%) was added *via* syringe. The reaction flask was cooled in an ice bath, and NaOH (5 mL, 3 M) was added dropwise followed by the dropwise addition of H_2O_2 (3 mL, 30%). This was allowed to stir for 15 min at 0 °C and then allowed to warm up to room temperature. Excess sodium thiosulfate was used to quench the reaction, and the crude product was extracted in ether (3 × 50 mL). The product was dried over magnesium sulfate and concentrated *in vacuo*. The GC and ^{1}H NMR showed two main products of >95% purity in a ratio of 7:3. Comparison with purchased materials showed 2-methoxyphenol (70%) and 3-methoxyphenol (30%).

X-ray Data Collection, Structure Determination, and Refinement. General Comments. A summary of the data collection parameters is given in Table 6. The crystals were mounted on a glass fiber. All measurements were made on an Enraf-Nonius CAD-4 diffractometer with graphite monochromated Mo Kα radiation. Cell constants, listed in Table 6, and an orientation matrix for data collection were obtained from a least-squares refinement using the setting angles of 25 carefully centered reflections in the range of $14.00 < 2\theta < 22.00°$.

The data were collected at −86 °C using the $\omega-2\theta$ scan technique. Moving crystal moving counter background measurements were made by scanning an additional 25% above and below the scan range. The counter aperture consisted of a variable horizontal slit with a width ranging from 2.0 to 2.5 mm and a vertical slit set to 2.0 mm. The diameter of the incident beam collimator was 0.7 mm, and the crystal to detector distance was 21 cm. For intense reflections an attenuator was automatically inserted in front of the detector.

An empirical absorption correction, using the program DIFABS,[23] was applied which resulted in the transmission factors listed in Table 6. The intensities were corrected for

---

[21] To measure the temperature, a thermometer was placed inside a sealable Schlenk tube (200 mL, 20 cm from the bottom to the seal) with 10 mL of THF. It was found that when the tube was immersed up to the level of the solvent in an oil bath set at 150 °C, the temperature of the THF was 110 °C.

[22] These experiments were also done in THF, and approximately the same ratios were observed.

Table 7. Atomic Coordinates and *B* Values (Å^2) for 3

atom	*x*	*y*	*z*	*B*(eq)
Zr	0.23690(4)	0.24212(2)	−0.00152(2)	1.54(1)
O(1)	0.4603(3)	0.2206(2)	0.0146(2)	1.8(1)
O(2)	0.0284(3)	0.3792(2)	−0.1646(2)	2.7(1)
C(1)	0.2416(6)	0.2876(3)	0.1588(3)	3.4(2)
C(2)	0.3100(5)	0.3604(4)	0.1224(3)	3.3(2)
C(3)	0.2053(7)	0.4036(3)	0.0566(3)	3.7(2)
C(4)	0.0759(5)	0.3574(4)	0.0535(3)	3.7(2)
C(5)	0.0981(5)	0.2876(4)	0.1157(3)	3.6(2)
C(6)	0.0154(5)	0.1469(4)	−0.0520(4)	3.9(2)
C(7)	0.0741(6)	0.1552(4)	−0.1271(3)	3.7(2)
C(8)	0.1988(7)	0.1086(5)	−0.1135(5)	5.3(3)
C(9)	0.2216(7)	0.0696(4)	−0.0311(7)	7.0(4)
C(10)	0.109(1)	0.0932(5)	0.0090(4)	6.3(3)
C(11)	0.4154(4)	0.3320(3)	−0.1209(2)	1.7(1)
C(12)	0.2679(4)	0.3306(3)	−0.1169(2)	1.7(1)
C(13)	0.1695(4)	0.3877(3)	−0.1749(3)	2.0(1)
C(14)	0.2119(5)	0.4467(3)	−0.2366(3)	2.2(2)
C(15)	0.3572(5)	0.4498(3)	−0.2394(3)	2.4(2)
C(16)	0.4564(4)	0.3947(3)	−0.1836(3)	2.2(2)
C(17)	0.5439(5)	0.1587(3)	0.0790(3)	2.7(2)
C(18)	0.5791(4)	0.1765(3)	−0.1213(3)	2.3(2)
C(19)	0.6820(4)	0.3186(3)	−0.0122(3)	2.3(2)
C(20)	0.6560(5)	0.2037(3)	−0.1959(3)	2.9(2)
C(21)	0.6635(5)	0.3905(3)	0.0586(3)	2.7(2)
C(22)	−0.0762(5)	0.4381(4)	−0.2181(4)	3.6(2)
B	0.5372(4)	0.2639(3)	−0.0623(3)	1.9(2)

Lorentz and polarization effects. A correction for secondary extinction was also applied. No decay corrections were required since the crystals displayed crystal and electronic stability.

The structure was solved using direct methods.[24] The non-hydrogen atoms were refined anisotropically.

Neutral atom scattering factors were taken from Cromer and Waber.[25] Anomalous dispersion effects were included in F_c; the values for $\Delta f'$ and $\Delta f''$ were those of Cromer.[26] All calculations were performed using the TEXSAN[27] crystallographic software package of Molecular Structure Corp.

X-ray Data Collection, Structure Determination, and Refinement for 3. On the basis of the systematic absences of $h0l$, $l \neq 2n$, and $0k0$; $k \neq 2n$, and the successful solution and refinement of the structure, the space group was determined to be $P2_1/c$.

The final cycle of full-matrix least-squares refinement was based on 2791 observed reflections ($I > 3.00\sigma(I)$) and 236 variable parameters and converged (largest parameter shift was 0.00 times its esd) with $R = 0.039$ and $R_w = 0.041$.

The standard deviation of an observation of unit weight was 3.64. The weighting Scheme was based on counting statistics and included a factor ($p = 0.02$) to downweight the intense reflections. Plots of $\sum w(|F_o| - |F_c|)^2$ *vs* $|F_o|$, reflection order in data collection, $(\sin \theta)/\lambda$, and various classes of indices showed no unusual trends. The maximum and minimum peaks on the final difference Fourier map corresponded to 0.41 and −0.58 e/Å^3, respectively.

The final values for refined coordinates of **3** are given in Table 7.

Table 8. Atomic Coordinates and *B* Values (Å^2) for 4

atom	*x*	*y*	*z*	*B*(eq)
Zr(1)	0.22144(8)	0.02010(4)	0.79061(4)	1.95(3)
O(1)	−0.0045(5)	0.0392(3)	0.8068(3)	3.2(3)
O(2)	−0.2068(5)	−0.0096(3)	0.6626(3)	2.7(2)
O(3)	−0.2144(5)	−0.1064(3)	0.7513(3)	2.8(2)
C(1)	0.190(1)	−0.0750(5)	0.9021(5)	3.9(4)
C(2)	0.301(1)	−0.1104(4)	0.8553(4)	3.5(4)
C(3)	0.442(1)	−0.0616(5)	0.8544(4)	3.3(4)
C(4)	0.410(1)	0.0028(5)	0.9031(5)	3.8(4)
C(5)	0.256(1)	−0.0047(5)	0.9310(4)	4.0(5)
C(6)	0.319(1)	0.0902(4)	0.6715(4)	3.5(4)
C(7)	0.200(1)	0.1389(4)	0.6996(5)	3.2(4)
C(8)	0.253(1)	0.1698(4)	0.7680(5)	3.6(4)
C(9)	0.407(1)	0.1403(5)	0.7832(5)	3.9(4)
C(10)	0.449(1)	0.0912(4)	0.7235(5)	3.6(4)
C(11)	0.0457(8)	−0.1035(4)	0.6693(4)	2.0(3)
C(12)	0.1938(8)	−0.0758(4)	0.6975(4)	1.7(3)
C(13)	0.3367(8)	−0.1109(4)	0.6681(4)	2.4(3)
C(14)	0.3358(9)	−0.1693(4)	0.6137(4)	2.5(3)
C(15)	0.1869(9)	−0.1982(4)	0.5844(4)	2.3(3)
C(16)	0.181(1)	−0.2587(5)	0.5286(4)	3.5(4)
C(17)	0.037(1)	−0.2848(5)	0.5000(5)	4.1(5)
C(18)	−0.109(1)	−0.2513(5)	0.5240(4)	3.8(4)
C(19)	−0.1064(9)	−0.1937(4)	0.5791(4)	2.9(4)
C(20)	0.0419(9)	−0.1649(4)	0.6112(4)	2.3(3)
C(21)	−0.144(1)	0.0607(8)	0.8419(7)	9.9(8)
C(22)	−0.150(1)	0.0325(5)	0.5982(5)	3.6(4)
C(23)	−0.164(1)	−0.1747(5)	0.7930(4)	3.4(4)
C(24)	−0.149(1)	0.1292(7)	0.8855(7)	8.0(7)
C(25)	−0.254(1)	0.0149(6)	0.5312(5)	6.2(6)
C(26)	−0.286(1)	−0.2412(5)	0.7822(5)	4.6(5)
B(1)	−0.126(1)	−0.0707(5)	0.6966(4)	2.1(4)
Zr(2)	0.22912(8)	0.51940(4)	0.71978(4)	1.82(3)
O(4)	0.4527(5)	0.5354(3)	0.6976(3)	2.5(2)
O(5)	0.6703(5)	0.4813(3)	0.8378(2)	2.2(2)
O(6)	0.6509(5)	0.3822(3)	0.7513(3)	2.7(2)
C(27)	0.134(1)	0.5889(4)	0.8392(4)	3.0(4)
C(28)	0.266(1)	0.6342(4)	0.8140(4)	3.1(4)
C(29)	0.224(1)	0.6693(4)	0.7444(5)	3.3(4)
C(30)	0.066(1)	0.6456(4)	0.7271(4)	3.0(4)
C(31)	0.0095(9)	0.5961(4)	0.7854(4)	2.9(4)
C(32)	0.172(1)	0.4948(5)	0.5809(4)	3.4(4)
C(33)	0.243(1)	0.4241(5)	0.6081(4)	3.3(4)
C(34)	0.137(1)	0.3884(4)	0.6595(4)	3.3(4)
C(35)	−0.0018(9)	0.4376(5)	0.6639(4)	3.0(4)
C(36)	0.021(1)	0.5014(4)	0.6141(4)	3.1(4)
C(37)	0.4052(8)	0.3938(4)	0.8410(4)	1.8(3)
C(38)	0.2577(8)	0.4238(4)	0.8143(4)	1.8(3)
C(39)	0.1124(8)	0.3922(4)	0.8467(4)	2.1(3)
C(40)	0.1144(8)	0.3364(4)	0.9024(4)	2.5(3)
C(41)	0.2615(8)	0.3051(4)	0.9306(4)	2.1(3)
C(42)	0.265(1)	0.2470(5)	0.9888(4)	3.4(4)
C(43)	0.409(1)	0.2187(5)	1.0164(5)	4.2(5)
C(44)	0.555(1)	0.2466(5)	0.9869(4)	3.8(4)
C(45)	0.5549(9)	0.3028(4)	0.9300(4)	2.9(4)
C(46)	0.4068(8)	0.3343(4)	0.9000(4)	2.0(3)
C(47)	0.597(1)	0.5564(6)	0.6627(5)	5.8(5)
C(48)	0.6320(9)	0.5255(4)	0.9035(4)	3.3(4)
C(49)	0.576(1)	0.3135(5)	0.7156(5)	4.3(5)
C(50)	0.588(1)	0.5980(7)	0.5942(6)	7.6(7)
C(51)	0.747(1)	0.5044(5)	0.9658(4)	4.0(4)
C(52)	0.644(3)	0.292(2)	0.648(1)	7(2)
C(52*)	0.715(3)	0.261(1)	0.694(2)	6(1)
B(2)	0.575(1)	0.4214(5)	0.8080(4)	1.9(4)

X-ray Data Collection, Structure Determination, and Refinement for 4. On the basis of systematic absences of $h0l$, $l \neq 2n$, and $0k0$, $k \neq 2n$, and the successful solution and refinement of the structure, the space group was determined to be $P2_1/c$.

The final cycle of full-matrix least-squares refinement was based on 4543 observed reflections ($I > 3.00\sigma(I)$) and 569 variable parameters and converged (largest parameter shift was 0.00 times its esd) with $R = 0.049$ and $R_w = 0.052$.

The standard deviation of an observation of unit weight was 1.43. The weighting Scheme was based on counting statistics and included a factor ($p = 0.02$) to downweight the intense reflections. Plots of $\sum w(|F_o| - |F_c|)^2$ *vs* $|F_o|$, reflection order in

---

(23) Walker, N.; Stuart, D. *Acta Crystallogr.* **1983**, *A39*, 158.

(24) (a) Gilmore, C. J. *J. Appl. Crystallogr.* **1984**, *17*, 42. (b) Beurskens, P. T. Direct Methods for Difference Structures—an automatic procedure for phase extension and refinement of difference structure factors, Crystallography Laboratory, Nijmegen, The Netherlands, 1984.

(25) Cromer, D. T.; Waber, J. T. *International Tables for X-Ray Crystallography*; The Kynoch Press: Birmingham, England, 1974; Vol. IV, Table 2.2.A.

(26) Cromer, D. T. *International Tables for X-Ray Crystallography*; The Kynoch Press: Birmingham, England, 1974; Vol. IV, Table 2.3.1.

(27) TEXSAN-TEXRAY Structure Analysis Package, Molecular Structure Corp., The Woodlands, TX.

data collection, (sin θ)/λ, and various classes of indices showed no unusual trends. The maximum and minimum peaks on the final difference Fourier map corresponded to 0.48 and −0.67 e/Å^3, respectively. Atomic Coordinates for **4** are found in Table 8.

Acknowledgment. This work was supported, in part, by a grant from the Office of Naval Research, who we gratefully acknowledge. We thank Dr. Daniel M. Giaquinta for help with the refinement of the crystal structure of **4**.

Supporting Information Available: Text describing crystallographic procedures and Tables of X-ray parameters, complete atom positional and thermal parameters, bond distances and angles, and torsion angles (56 pages). Ordering information is given on any current masthead page.

OM950278D